Ancient DNA and morphometric analysis reveal extinction and replacement of New Zealand's unique black swans

Nicolas J. Rawlence[#], Afroditi Kardamaki[#], Luke J. Easton, Alan J. D. Tennyson, R. Paul Scofield, Jonathan M. Waters

[#] Equal first authors

Supplementary Information

1. Materials and Methods

(a) Osteology and morphometric analysis

We recorded 24 length (total length, L) and width (proximal width, PW; shaft width, SW; and distal width, DW) measurements, defined by von den Driesch [1], of postcranial elements including coracoids (cor, L and DW only), humeri (hum), ulnae (ulna), carpometacarpi (cmc, L and PW only), femora (fem), tibiotarsi (tt) and tarsometatarsi (tmt) from associated osteologically mature skeletons or partial skeletons of modern (Australian) *Cygnus atratus*, and prehistoric New Zealand (NZ) and Chatham Islands (CI) black swans (including the holotype of *C. s. chathamicus* Oliver, 1955 NMNZ S.23219; see Table S2). We also recorded 11 cranial measurements, defined by von den Driesch [1], from associated osteologically mature skeletons and isolated crania of modern (Australian) *C. atratus*, and prehistoric NZ and CI black swans (Table S2) – many from the same specimens as for postcranial analysis. There was no measurable cranial material for prehistoric NZ black swans, and as such cranial material of the morphologically and genetically closely related CI black swan lineage (Fig. 1) is used as a proxy for the prehistoric NZ lineage (*cf. Corvus* ravens [2]). Overall, we obtained measurements from 25 partial skeletons, 20 partial postcranial skeletons and 16 crania for modern (Australian) *C. atratus*; six partial postcranial skeletons of the prehistoric NZ black swan; and nine partial skeletons, 11 partial postcranial skeletons and 21 crania for the prehistoric CI black swan.

The cranial measurements are defined as follows:

GBP: Greatest breadth across the processus postfrontales.

GL: Greatest length from the protuberantia occipitalis externa to the apex praemaxillaris.

SBO: Smallest breadth between the orbits on the dorsal side (smallest breadth of the pars nasalis of the frontale).

PSL: Breadth across the processus supraorbitalis of the lacrimal (upper part).

NL: Greatest length of the nasal cavity.

AND: Greatest depth of maxilla at the anterior end of the nasal cavity.

AWNL: Breadth of maxilla across the anterior end of the nasal cavity.

ABL: Greatest breadth across the anterior end of the maxilla.

CFCF: Length from prominentia cerabellus (terminal cranial process) to fissura cranio-facialis.

FCF-AB: Length from fissura cranio-facialis to anterior tip of maxilla.

MD: Greatest depth of mandible.

Measurements were taken using Vernier callipers to the nearest 0.1 mm, using techniques defined by von den Driesch [1]. Specimens were housed in Auckland Museum (AM), National Museum of New Zealand Te Papa Tongarewa (NMNZ), Canterbury Museum (CM), Otago Museum (OM), and the University of Otago Archaeology and Anthropology Department (OUAD). Only non-weathered bones where accurate length measurements could be obtained were analysed to avoid taphonomic biases influencing the results [3].

Morphological differentiation and diagnosibility between modern (Australian) and prehistoric (NZ/CI) genetic lineages (see Fig. 1) were tested utilising the complete, cranial and postcranial datasets in a principal component analysis (PCA) and discriminant function analysis (DFA) framework in R [4]. PCA and DFA analyses utilised the prcomp and lda functions in R, respectively. Missing values were replaced within each dataset (i.e. not across datasets) and lineage (i.e. modern Australian, prehistoric NZ, prehistoric CI) using predictive matching means in the R package MICE [5] – specimens with too many missing values, as determined by MICE, were excluded from the imputated datasets (Tables S3-5). The MICE algorithm imputes an incomplete column (the target column) by generating 'plausible' synthetic values given other columns in the dataset. Each incomplete column must act as a

target column, and has its own specific set of predictors. The default set of predictors for a given target consists of all other columns in the dataset [5-7]. Eigenvalues were examined to determine which axis and variables contributed the most information.

Simpson's log-ratio was utilised to test for differences in mean postcranial element lengths (i.e. 'island rule' effects) amongst modern (Australian) and prehistoric (NZ/CI) lineages [8]. The logarithmic differences of the mean postcranial element lengths (using the iterative imputated datasets) of the CI lineage (proxy for NZ lineage due to small sample size *cf. Corvus* spp. [2]) and combined NZ/CI lineages, relative to the modern (Australian) lineage, were calculated in Excel. These logarithmic differences were subsequently imported into R to construct Fig. 2B.

The flight ability (flightless, flight-reduced or volant) of prehistoric (NZ/CI) swans was assessed following the methodology of Watanabe [9] which statistically compares the flight ability of extinct Anatidae on the basis of known flightless and volant (e.g. modern Australian black swan) taxa. Mean morphometric length measurements were restricted to hum, ulna, cmc, fem and tmt, whereas tt was excluded from the analysis because swan measurements (total length) were not comparable to measurements of [9] (tt length excluding cnemial crest). Morphometric analysis was restricted to modern (Australian) and prehistoric (NZ/CI) swans, and known flightless Anatidae (data sourced from [9]) using PCA in R (as opposed to Linear Discriminant Analysis, as this method produces a binary (flightless, volant) score but gives no indication of flight-reduction; [9]).

Mean body mass of *Cygnus* individuals was reconstructed using tt SW measurements, and the Anatidae body mass reference dataset of Dickison [10]. Tibiotarsus SW (in mm) of prehistoric (NZ/CI) and modern (Australian) associated *Cygnus* skeletons was converted into tt circumference using the formula $C = 2\pi r$ in Excel using the iterative imputated complete and postcranial datasets. We included anatid tt circumference/body mass reference data from Dickison [10] (see Table 3.1 of [10]), covering the phylogenetic and size range of extant anatids, to model the mean predicted weight of each *Cygnus* lineage. Modelling was conducted in R using a modified version of Dickison [10] Table 3.2 formula for Least Squares regression of body mass (y, in grams) on anatid bone measurements. Dickinson [10] formula is $y = a \times x^b$. We modified this formula ($y = a + x^b$) to regress body weight against tt circumference, with 'a' (intercept = 330 g), '*x*' (circumference) and 'b' (exponential scaling factor = 2.526). The use of this modified formula and tt circumference (as opposed to femoral

circumference) was to obtain predicted mean weights of modern (Australian) *Cygnus* in the range of 5-6 kg (matching that known for recently dead birds; [11]) as swans are a highly derived form of anatid compared to ducks and geese. Our revised formula predicted the weight of the extinct South Island goose (*Cnemiornis calcitrans*) within the range predicted by Dickison [10], therefore we are confident of the reliability of our formula.

2. Results:

(a) PCA/DFA of complete Cygnus *skeletons*

Principal Component Analysis (PCA) analysis of complete (cranial and postcranial) skeletons of modern (Australian) and prehistoric (CI – proxy for NZ in the absence of measurable cranial material) *Cygnus* showed pronounced morphometric divergence (Fig. S2), and 100% diagnosability (Fig. S3). High positive PC1 loadings were seen for all cranial and postcranial elements (length and width measurements) indicating prehistoric (NZ/CI) *Cygnus* are overall larger than modern (Australian) black swans. Negative PC2 loadings (Hum DW - 0.35, Ulna PW -0.33) indicate modern (Australian) *Cygnus* are more gracile than prehistoric (NZ/CI) black swans. Positive PC2 loadings on cranial elements (NL 0.27, FCF-AB 0.26) indicate that prehistoric (NZ/CI) *Cygnus* have more elongate skulls compared to modern (Australian) black swans.

(b) PCA/DFA of Cygnus *crania*

In contrast to PCA and DFA analyses of complete (cranial and postcranial) *Cygnus* skeletons, the PCA distributions of modern (Australian) and prehistoric (CI – proxy for NZ due to the absence of measurable cranial material) are fully overlapping (Fig. S4). However, the positive PC1 outlier is morphologically confirmed as a modern (Australian) *C. atratus* and therefore represents the extreme upper end of the size range for this species. If this morphometric outlier is ignored, there is minimal overlap between modern (Australian) and prehistoric (NZ/CI) black swans. Positive PCA loadings on all cranial elements (lengths and widths) indicate that prehistoric (NZ/CI) *Cygnus* had larger and more robust crania than the more gracile modern (Australian) black swans. In spite of the morphometric overlap shown in Fig. S4, there was 100% diagnosibility of modern (Australian) and prehistoric (NZ/CI) individuals (Fig. S5).

(c) PCA/DFA of Cygnus *postcranial skeletons*

Principal Component Analysis showed clear morphometric divergence (with minimal overlap) of modern (Australian) and prehistoric (NZ/CI) black swans (Fig. 2A). Negative PC1 loadings on all postcranial elements (lengths and widths) indicates that modern (Australian) *Cygnus* are on average smaller than prehistoric (NZ/CI) black swans. Positive (Hum SW 0.46, Fem SW 0.34) and negative (Hum L -0.37; Ulna PW -0.35) PC2 loadings indicate that prehistoric (NZ/CI) black swans have more robust (larger and wider) wings and legs compared to modern (Australian) *Cygnus*. We also detected pronounced morphological substructure amongst prehistoric NZ and CI black swans, with relatively more robust humeri and femora detected in prehistoric mainland NZ *Cygnus* (Fig. 2A).

Discriminant Function Analysis showed high diagnosibility between modern (Australian) and prehistoric (NZ/CI) *Cygnus* (Fig. S6): 98% for modern (Australian), 100% for prehistoric CI, and 67% for prehistoric NZ – this equates to only one modern (Australian) individual (CM Av7322) mis-diagnosed as a prehistoric NZ *Cygnus*, and two prehistoric NZ individuals (NMNZ S.5504, CM Av12571) mis-diagnosed as prehistoric CI *Cygnus*. Despite the absence of cranial material for these specimens, a previous study on morphometrics of NZ birds [12] showed that similar misdiagnoses in DFA analyses of cranial or postcranial skeletons are not seen when complete skeletons are analysed in a DFA framework, especially in species where there is overlapping size distributions between taxa.

(d) Simpson's log ratio of Cygnus *postcranial skeletons*

Simpon's log ratio of postcranial elements indicated that size differences between modern (Australian) and prehistoric (NZ/CI) detected in the PCA analysis (Fig. 2A), were particularly pronounced for hind limb elements (i.e. femora, tibiotarsi and tarsometatarsi). Bones from prehistoric CI (proxy for prehistoric NZ due to the small sample size [six postcranial skeletons] from mainland NZ *cf. Corvus* spp.; [2]) were highly elongated relative to those from modern (Australian) black swans (Fig. 2B). This contrast is highlighted by distinct tarsometatarsus to femur ratios (Fig. 2B).

The inclusion of prehistoric NZ black swan postcranial elements in the CI dataset did result in a decrease in the Simspon's log ratio of humeri, ulna and carpometacarpi (*cf.* to coracoid) (Fig. S7). The decrease in log ratio for these postcranial elements is no doubt due to the small sample size of prehistoric NZ black swans available for analysis. However, log ratios for the combined prehistoric (NZ/CI) black swans were still larger than modern

(Australian) *Cygnus*, indicating that overall prehistoric NZ/CI black swans are larger than modern (Australian) individuals, with pronounced elongation of the leg bones.

(e) Flight ability of prehistoric (NZ/CI) Cygnus

Assessment of flight ability (flightless, flight-reduced, or volant) using PCA suggest that prehistoric (NZ/CI) swans were likely flight-reduced compared to volant modern (Australian) black swans. Specifically, principal component loadings indicated significant elongation of the hind limbs (PC1: fem 0.42; tmt 0.45) and proportionally shorter wing bones in relation to hind limbs in prehistoric (NZ/CI) swans (PC2: hum -0.26; ulna -0.37; cmc -0.41; fem 0.65 and tmt 0.44). These findings are congruent with morphometric analyses (Fig. 2) showing that the wing bones of prehistoric (NZ/CI) individuals were more robust than modern (Australian) black swans.

(f) Reconstructing body mass of prehistoric (NZ/CI) Cygnus

Reconstructing body mass (mean weight in kg) from femoral shaft width (Fig. S9 *cf.* tibiotarsus shaft width, Fig. 2C), did not produce mean weights of modern (Australian) *C. atratus* in the range of 5-6 kg, as have been reported for recently dead birds [8]. Swans have asymmetrical long bone shafts that are relatively narrow, therefore the simple SW measurement may not predict shaft circumference well and hence our modification of the scaling formula. Body mass reconstructions using tibiotarsus shaft width show prehistoric (NZ/CI) *Cygnus* to be 20-32% heavier than those from modern (Australian) populations (Fig. 2C), with weights ranging from 6-10 kg, compared to 4-9 kg for modern (Australian) individuals: mean weights were 5.75 kg (4.11-8.93 kg) for modern (Australian) *C. atratus*, 6.93 kg (6.37-7.67 kg) for prehistoric NZ *Cygnus*, and 8.40 kg (7.11-9.71 kg) for prehistoric CI *Cygnus* (See Table S6).

3. Discussion

(a) Species concepts and taxonomic implications

The combined genetic, morphometric and palaeoecological data support recognition of the modern (Australian) and prehistoric (NZ and CI) black swans as separate species under the diagnosable species concept (DSC) [13-16]. Furthermore, genetic and morphometric data support recognition of the prehistoric NZ and CI lineages as separate subspecies under the DSC. This view of species is a derivative of the phylogenetic species concept [17], designed

to avoid taxonomic over-inflation [13, 18] and rejects Helbig's et al. [14] allospecies, semispecies and superspecies concepts (see Gill et al. [19] for discussion). Though not universally accepted [20-22] our use of the DSC is the approach advocated by Birds NZ (Ornithological Society of New Zealand Checklist Committee; [19]). We cannot apply the Biological Species Concept (BSC) [23-24] as the modern (Australian) and prehistoric (NZ and CI) lineages are allopatric, with the latter lineage extinct. The BSC is highly problematic in birds with widespread interspecific and intergeneric hybridisation and paraphyly in good biological species [25-27]. It would be possible to further test the presence of two species within black swans in future research, through high-throughput sequencing utilising single-stranded library preparation and hybridisation capture-enrichment techniques specifically designed for ancient DNA [28-29]. Although species delimitation based on single-marker gene trees (*sensu* [30]) should be treated with caution [31], the 335 bp of mtDNA *CR* utilised in this study (containing 25 parsimony informative sites) does show that multiple lineages are present within black swans that are diagnosably distinct based on morphology and palaeobehaviour. Alternative taxonomic hypotheses are not supported by our data. The combined genetic, morphometric and palaeoecological data rejects the hypothesis of a single black swan species across Australasia. Likewise, the genetic substructure within the prehistoric NZ lineage (one fixed SNP between NZ and CI swans), despite pronounced morphological substructure (more robust humeri and femora in prehistoric mainland NZ black swans) does not support the hypothesis of three species of black swan.

References

1. von den Driesch A. 1976 *A guide to the measurements of animal bones from archaeological sites*. Peabody Museum Bulletin 1.

2. Scofield RP, Mitchell KJ, Wood JR, de Pietri VL, Jarvie S, Llamas B, Cooper A. 2017 The origin and phylogenetic relationships of the New Zealand ravens. *Mol. Phylo. Evol.* **106**, 136–143.

3. Worthy TH. 1998 A remarkable fossil and archaeological avifauna from Marfells Beach, Lake Grassmere, South Island, New Zealand. *Rec. Cant. Mus.* **12**, 79–176.

4. R Development Core Team. 2008 R: *A Language and Environment for Statistical Computing*. Vienna: R Foundation for Statistical Computing.

5. van Buuren S, Groothuis-Oudshoorn G. 2011 MICE: Multivariate imputation by chained equations in R. *J. Stat. Soft.* **45**, 29864.

6. Schenker N, Taylor JMG. 1996 Partially parametric techniques for multiple imputation. *Comp. Stat. Data Anal.* **22**, 425-446.

7. Clavel J, Merceron G, Escarguel G. 2014 Missing data estimation in morphometrics: how much is too much? *Syst. Biol.* **63**, 203-218.

8. Wood JR, Mitchell KJ, Scofield RP, de Pietri VL, Rawlence NJ, Cooper A. 2017 Phylogenetic relationships and terrestrial adaptations of the extinct laughing owl, *Sceloglaux albifacies* (Aves: Strigidae). *Zoo. J. Linn. Soc.* **179**, 907-918.

9. Watanabe J. 2017 Quantitative discrimination of flightlessness in fossil Anatidae from skeletal proportions. *Auk Ornith. Advan.* **134**, 672-695.

10. Dickison MR. 2007 *The allometry of giant flightless birds*. Unpublished PhD thesis, Duke University.

11. Marchant S, Higgins PJ. 1990 *Handbook of Australian, New Zealand and Antarctic birds*, volume 1, part B pelican to ducks. Melbourne: Oxford University Press.

12. Rawlence NJ, Scofield RP, Spencer HG, Lalas C, Easton KJ, Tennyson AJD, Adams M, Pasquet E, Fraser C, Waters JM, Kennedy M. 2016 Genetic and morphological evidence for two species of *Leucocarbo* shag (Aves, Pelecaniformes, Phalacrocoracidae) from southern South Island of New Zealand. *Zoo. J. Linn. Soc.* **177**, 676–694.

13. Baum DA, Donoghue MJ. 1995 Choosing among alternative "phylogenetic" species concepts. *Syst. Bot.* **20**, 560–573.

14. Helbig AJ, Knox AG, Parkin DT, Sangster G, Collinson M. 2002 Guidelines for assigning species rank. *Ibis* **144**, 518–525.

15. Patten MA, Unitt P. 2002 Diagnosability versus mean differences of sage sparrow subspecies. *Auk* **119**, 26–35.

16. Cicero C, Johnson NK. 2006 Diagnosability of subspecies: lessons from sage sparrows (*Amphispiza belli*) for analysis of geographic variation in birds. *Auk* **123**, 266–274.

17. Cracraft J. 1983 Species concepts and speciation analysis. *Curr. Ornith.* **1**, 159–187.

18. Issac NJB, Mallet J, Mace GM. 2004 Taxonomic inflation: its influence on macroecology and conservation. *Trends Ecol. Evol*. **19**, 464–469.

19. Gill BJ, Bell BD, Chambers GK, Medway DG, Palma RL, Scofield RP, Tennyson AJD, Worthy TH. 2010 *Checklist of the Birds in New Zealand, Norfolk and Macquarie Islands, and the Ross Dependency Antarctica*, 4th edn. Wellington: Te Papa Press in association with the Ornithological Society of New Zealand.

20. Tobias JA, Seddon N, Spottiswoode CN, Pilgrim JD, Fishpool LDC, Collar NJ. 2010 Quantitative criteria for species delimitation. *Ibis* **152**, 724–726.

21. Gill FB. 2014 Species taxonomy of birds: which null hypothesis? *Auk* **131**, 150–161.

22. Toews DPL. 2014 Biological species and taxonomic species: will a new null hypothesis help? (A comment on Gill 2014). *Auk* **132**, 78–81.

23. Mayr E. 1940 Speciation phenomena in birds. *Amer. Nat.* **74**, 249–278.

24. Mayr E. 1996 What is a species and what is not? *Phil. Sci.* **63**, 261–276.

25. Grant PR, Grant BR. 1992 Hybridization of bird species. *Science* **256**, 193–197.

26. Grant PR, Grant BR. 1997 Genetics and the origin of bird species. *PNAS* **94**, 7768–7775.

27. Joseph L, Omland KE. 2009 Phylogeography: its development and impact in Australo-Papuan ornithology with special reference to paraphyly in Australian birds. *Emu* **109**, 1–23.

28. Gansauge MT, Meyer M. 2013 Single-stranded DNA library preparation for the sequencing of ancient or damaged DNA. *Nat. Proto.* **8**, 737–748.

29. Mitchell KJ, Wood JR, Scofield RP, Llamas B, Cooper A. 2014 Ancient mitochondrial genome reveals unsuspected taxonomic affinity of the extinct Chatham duck (*Pachyanas chathamica*) and resolves divergence times for New Zealand and sub-Antarctic brown teals. *Mol. Phylo. Evol.* **70**, 420–428.

30. Edwards SV. 2009 Is a new and general theory of molecular systematics emerging? *Evolution* **63**, 1–19.

31. Carstens BC, Pelletier TA, Reid NM, Satler JD. 2013 How to fail at species delimitation. *Mol. Ecol.* **22**, 4369–4383.

Table S1 Ancient, historic and modern *Cygnus* specimens used for genetic analysis. Abbreviations are as follows: NMNZ, Museum of New Zealand Te Papa Tongarewa; CM, Canterbury Museum; JH, Jill Hamel Collection; AM, Auckland Museum; OZD, Otago University Zoology Department; OM, Otago Museum; WAM, Western Australian Museum; SAM, South Australian Museum; MV, Museum Victoria; ANWC, Australian National Wildlife Collection, CSIRO, Canberra; QM, Queensland Museum; NZ, New Zealand; WA, Western Australia; NT, Northern Territory; SA, South Australia; TAS, Tasmania; VIC, Victoria; NSW, New South Wales; ACT, Australian Capital Territory; QLD, Queensland.

Species (based on DNA and morphology)	Museum accession no.	Geographic location	Age	GenBank No.
C. s. sumnerensis	NMNZ S.40879	Manurewa Pt.	<2000 yrs BP – 1450 AD	MF455394
C. s. sumnerensis	CM Av16010	Wairau Bar	1280-1450 AD	MF455451
C. s. sumnerensis	CM Av25624	Wairau Bar	1280-1450 AD	MF455452
C. s. sumnerensis	CM Av16000	Wairau Bar	1280-1450 AD	MF455450
C. s. sumnerensis	CM Av12865	Marfells Beach	<1500 yrs BP-1450 AD	MF455379
C. s. sumnerensis	CM Av12423	Marfells Beach	<1500 yrs BP-1450 AD	MF455447
C. s. sumnerensis	CM Av11901	Marfells Beach	<1500 yrs BP-1450 AD	MF455448
C. s. sumnerensis	CM Av10601a	Lake Grassmere	<1500 yrs BP-1450 AD	MF455446
C. s. sumnerensis	CM Av9650	Lake Grassmere	<1500 yrs BP-1450 AD	MF455380
C. s. sumnerensis	CM Av16260	Redcliffs	1280-1450 AD	MF455449
C. s. sumnerensis	JH HW105	Harwood	<2000 yrs BP-1450 AD	MF455384
C. s. sumnerensis	JH HW23 (Grey)	Harwood	<2000 yrs BP-1450 AD	MF455385
C. s. sumnerensis	JH HW23 (Brown)	Harwood	<2000 yrs BP-1450 AD	MF455386
C. s. sumnerensis	CM Av34804	Pounawea	1280-1450 AD	MF455381
C. s. sumnerensis	CM Av34794	Pounawea	1280-1450 AD	MF455382
C. s. sumnerensis	CM Av32919	Pounawea	1280-1450 AD	MF455383
C. s. sumnerensis	NMNZ S.32994	Chatham Islands	Late Holocene	MF455435
C. s. chathamicus	NMNZ S.26438	Tahatika Stream, Chatham Is.	Late Holocene	MF455387
C. s. chathamicus	NMNZ S.25083	Tahatika Creek, Chatham Is.	Late Holocene	MF455388
C. s. chathamicus	CM Av5288	Chatham Is.	Late Holocene	MF455437
C. s. chathamicus	CM Av5289	Chatham Is.	Late Holocene	MF455438
C. s. chathamicus	CM Av3314	Chatham Is.	Late Holocene	MF455439
C. s. chathamicus	CM Av5391	Chatham Is.	Late Holocene	MF455440
C. s. chathamicus	CM Av6493.2	Chatham Is.	Late Holocene	MF455441
C. s. chathamicus	CM Av5307.10	Chatham Is.	Late Holocene	MF455442
C. s. chathamicus	CM Av6493.3	Chatham Is.	Late Holocene	MF455443
C. s. chathamicus	NMNZ S.36074	Waitangi West, Chatham Is.	Late Holocene	MF455389
C. s. chathamicus	NMNZ S.29964	Tupuangi Creek, Pitt Is.	1450-1650 AD	MF455390
C. s. chathamicus	NMNZ S.29761	Tupuangi Creek, Pitt Is.	1450-1650 AD	MF455391
C. s. chathamicus	NMNZ S.31490	Tupuangi Creek, Pitt Is.	1450-1650 AD	MF455392

C. s. chathamicus	NMNZ S.35332	North Head, Pitt Is.	Late Holocene	MF455393
C. s. chathamicus	CM Av6493.1	Chatham Islands	Late Holocene	MF455398
C. s. chathamicus	NMNZ S.23219	Chatham Islands	Late Holocene	MF455431
C. s. chathamicus	NMNZ S.26457	Tahatika Creek, Chatham Is.	Late Holocene	MF455432
C. s. chathamicus	NMNZ S.28867	Tahatika Creek, Chatham Is.	Late Holocene	MF455433
C. s. chathamicus	NMNZ S.33001	Tahatika Creek, Chatham Is.	Late Holocene	MF455434
C. s. chathamicus	NMNZ S.26979	Tahatika Creek, Chatham Is.	Late Holocene	MF455436
C. atratus	AM LB216	Waikaremoana Cave, NZ	1450 AD-1800's	MF455445
C. atratus	NMNZ S.46032	Waikaremoana Cave, NZ	1450 AD-1800's	MF455444
C. atratus	NMNZ OR.16629	Awatapu Lagoon, NZ	1972	MF455395
C. atratus	NMNZ OR.16641	Lake Rotorua, NZ	1971	MF455396
C. atratus	OZD AA63	Wairarapa, NZ	Modern	MF455419
C. atratus	NMNZ OR.29671	Pauatahanui Stream, NZ	Modern	MF455420
C. atratus	OZD AA60	All Day Bay, NZ	Modern	MF455416
C. atratus	OZD AA61	All Day Bay, NZ	Modern	MF455417
C. atratus	OZD AA62	All Day Bay, NZ	Modern	MF455418
C. atratus	OM AV909	Hawksbury Lagoon, NZ	Modern	MF455430
C. atratus	NMNZ OR.29960	Blind Jims Creek, Chatham Is.	Modern	MF455397
C. atratus	CM Av30460	Chatham Is.	Modern	MF455453
C. atratus	OZD CI1	Chatham Is.	Modern	MF455454
C. atratus	OZD CI2	Chatham Is.	Modern	MF455455
C. atratus	OZD CI3	Chatham Is.	Modern	MF455456
C. atratus	OZD CI4	Chatham Is.	Modern	MF455457
C. atratus	OZD CI5	Chatham Is.	Modern	MF455458
C. atratus	OZD CI6	Chatham Is.	Modern	MF455459
C. atratus	OZD CI7	Chatham Is.	Modern	MF455460
C. atratus	OZD CI8	Chatham Is.	Modern	MF455461
C. atratus	OZD CI9	Chatham Is.	Modern	MF455462
C. atratus	SAM ABTC2814	Adelaide, SA	Modern	MF455399
C. atratus	SAM ABTC2857	Southeast SA	Modern	MF455400
C. atratus	SAM ABTC127893	SA	Modern	MF455401
C. atratus	SAM ABTC81555	VIC	Modern	MF455402
C. atratus	SAM ABTC67801	Eyre Penn., SA	Modern	MF455403
C. atratus	SAM ABTC28716	NT	Modern	MF455404
C. atratus	QM A002725	Warner, Brisbane, QLD	Modern	MF455405
C. atratus	QM A002811	Brendale, Brisbane, QLD	Modern	MF455406
C. atratus	ANWC B50124	Mullawoolka Basin, NSW	Modern	MF455407
C. atratus	ANWC B50086	Gulpa Creek, NSW	Modern	MF455408
C. atratus	ANWC B45489	Bells Lagoon, TAS	Modern	MF455409
C. atratus	ANWC B45490	Bells Lagoon, TAS	Modern	MF455410
C. atratus	ANWC B50182	Mullawoolka Basin, NSW	Modern	MF455411
C. atratus	ANWC B53612	Lake Burley Griffin, ACT	Modern	MF455412
C. atratus	ANWC B50277	Big Poorrarecup Lake, WA	Modern	MF455413
C. atratus	ANWC B50245	Esperance, WA	Modern	MF455414
C. atratus	ANWC B50405	Lake Namming, WA	Modern	MF455415
C. atratus	MV 7291	Albert Park Lake, Melbourne, VIC	Modern	MF455421
C. atratus	MV 7292	Edithvale Wetlands, VIC	Modern	MF455422
C. atratus	MV 11230	Patterson Lakes, VIC	Modern	MF455423

C. atratus	MV 2075	Orbost, VIC	Modern	MF455424
C. atratus	WAM TA373	Lake Monger Wembley, WA	Modern	MF455425
C. atratus	WAM TA374	Lake Monger Wembley, WA	Modern	MF455426
C. atratus	WAM TA376	Lake Monger Wembley, WA	Modern	MF455427
C. atratus	WAM TA385	Lake Joondalup, WA	Modern	MF455428
C. atratus	WAM PR3500	Lake Monger, WA	Modern	MF455429
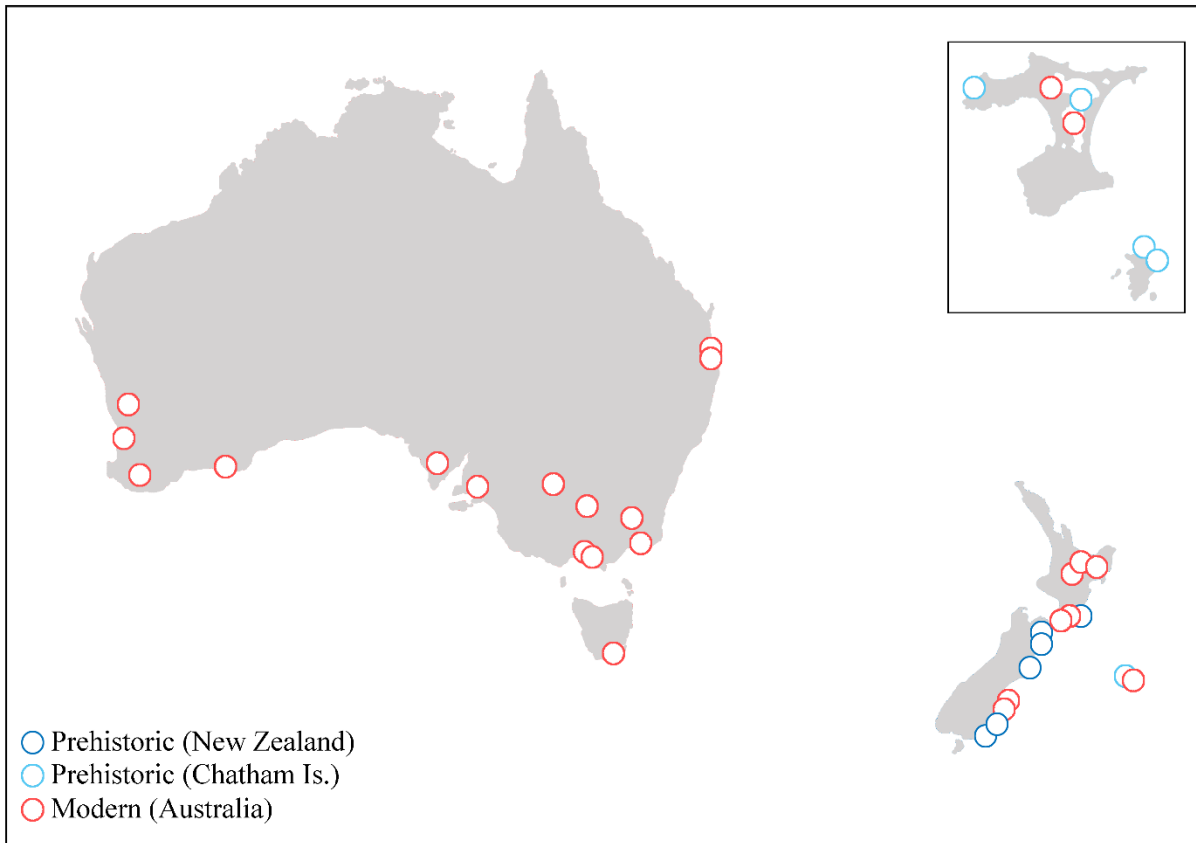
Figure S1 Geographic and temporal distribution of *Cygnus* samples analysed in this study. Insert: Chatham Islands. Modern (Australian) black swans with sampling locations of Northern Territory, South Australia, southeast South Australia and Victoria are not shown in Figure 1.
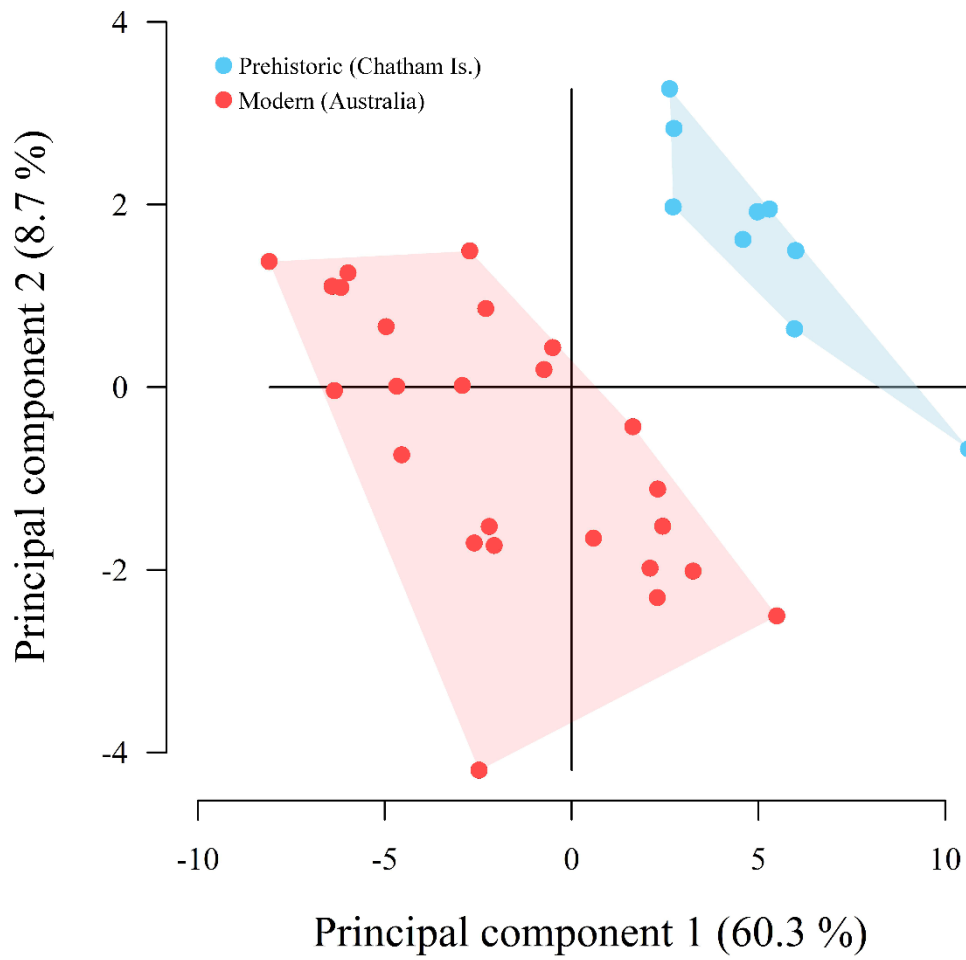
Figure S2 Principal Component Analysis of pooled cranial and postcranial measurements of modern (Australian) and prehistoric (CI – proxy for NZ) *Cygnus* swans.
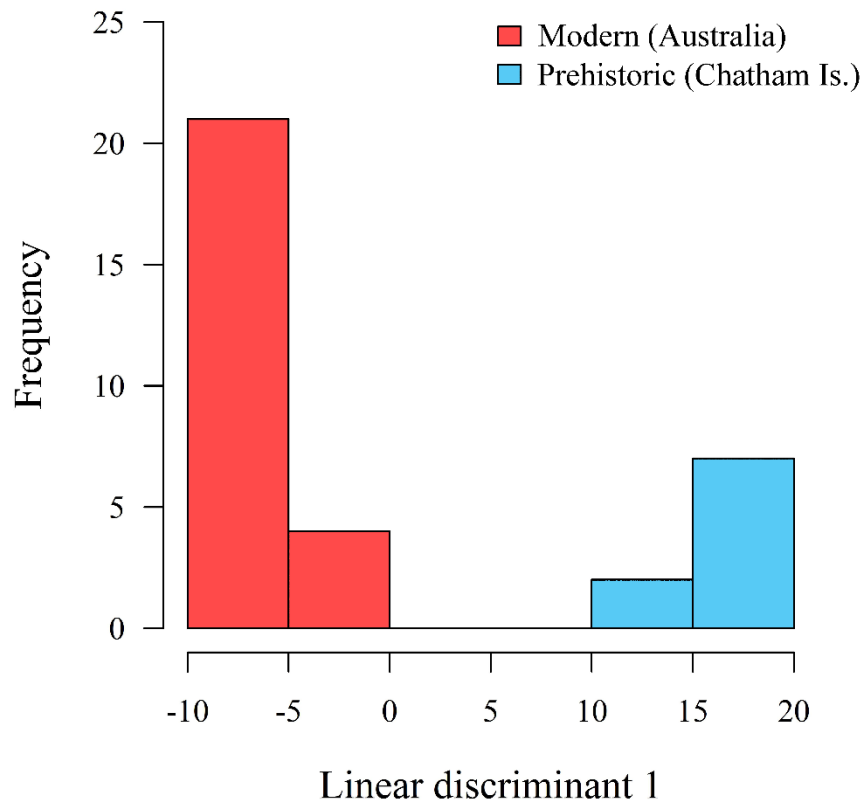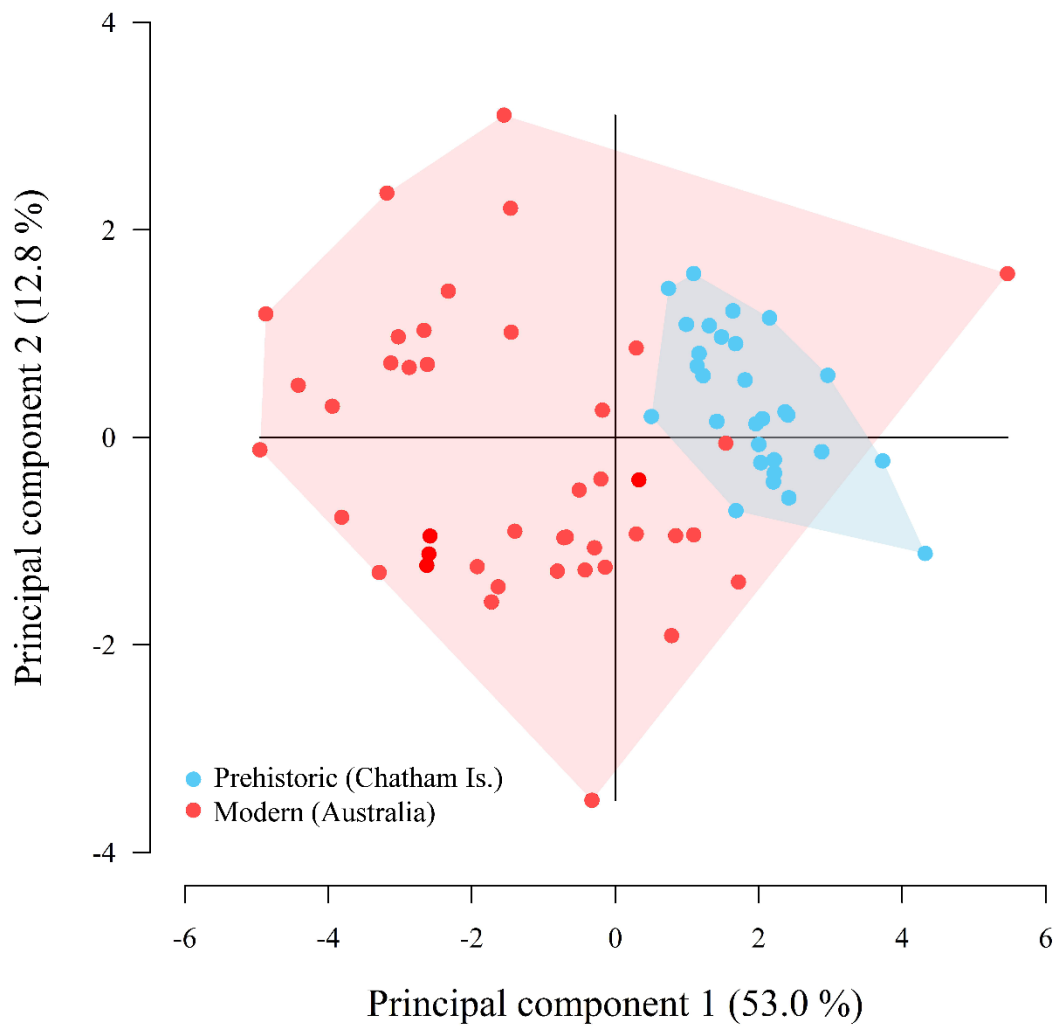
Figure S3 Discriminant Function Analysis of pooled cranial and postcranial measurements of modern (Australian) and prehistoric (CI – proxy for NZ) *Cygnus* swans.

Figure S4 Principal Component Analysis of cranial measurements of modern (Australian) and prehistoric (CI – proxy for NZ) *Cygnus* swans.
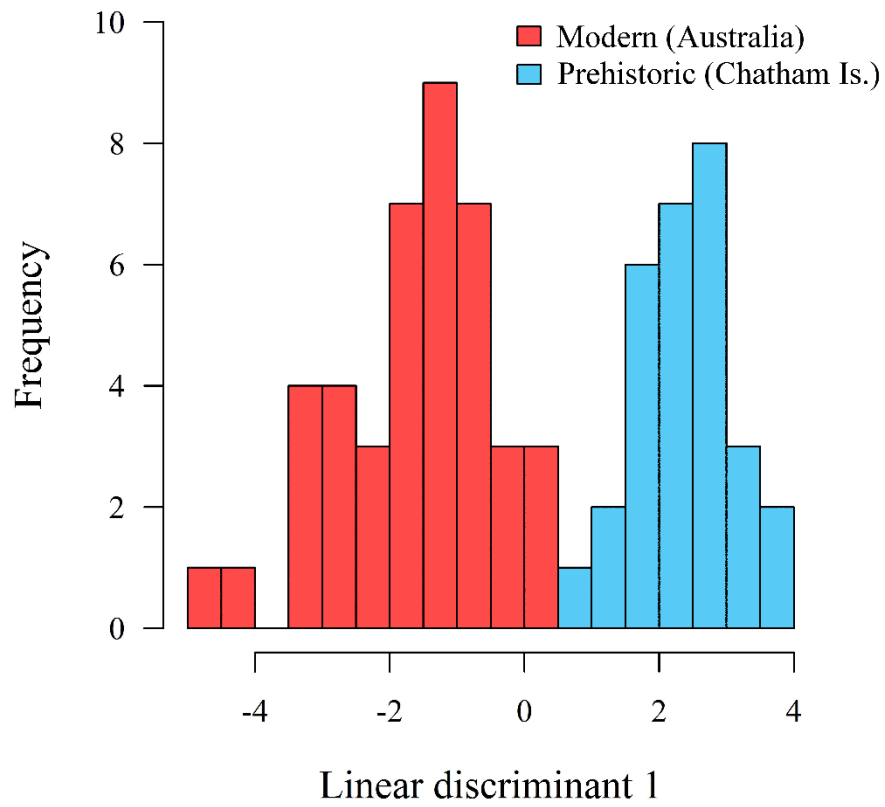
Figure S5 Discriminant Function Analysis of cranial measurements of modern (Australian) and prehistoric (CI – proxy for NZ) *Cygnus* swans.
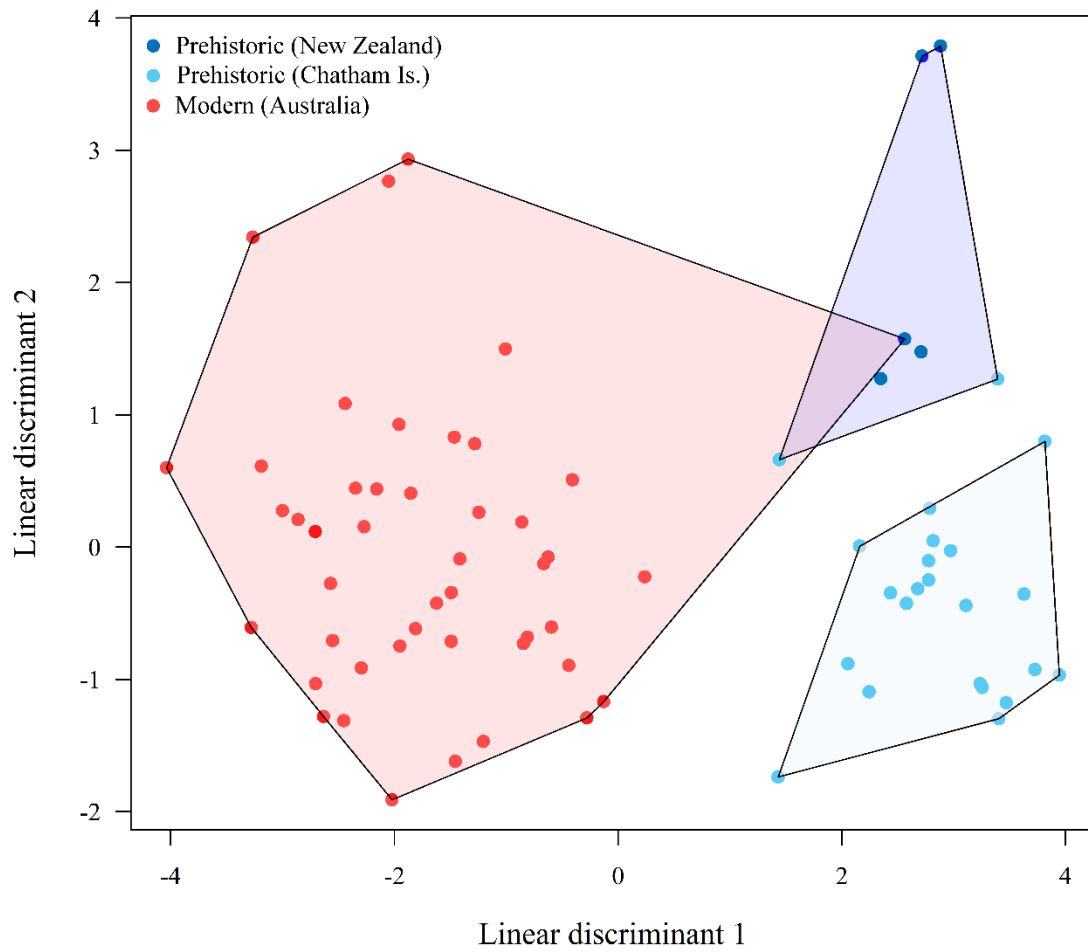
Figure S6 Discriminant Function Analysis of postcranial skeletons of modern (Australian) and prehistoric (NZ/CI) *Cygnus* swans. The convex hulls represent the morphometric distribution of each genetic lineage, while the colours of the dots represent the morphometric diagnosis as determined by DFA.
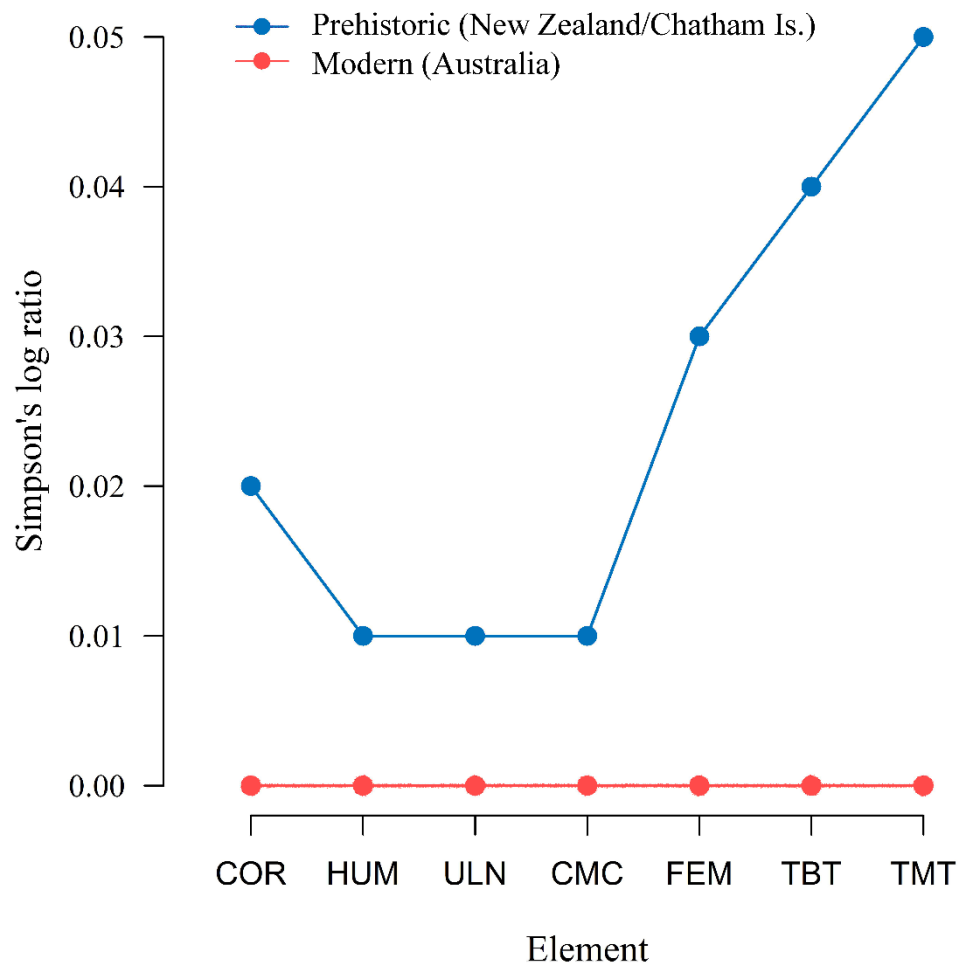
Figure S7 Simpson's log-ratio diagram, showing the logarithmic differences of mean lengths of the postcranial elements of prehistoric *Cygnus* from New Zealand and the Chatham Islands relative to the modern (Australian) *Cygnus*. Abbreviations: COR, coracoid; HUM, humerus; ULN, ulna; CMC, carpometacarpus; FEM, femur, TBT, tibiotarsus; TMT, tarsometatarsus.
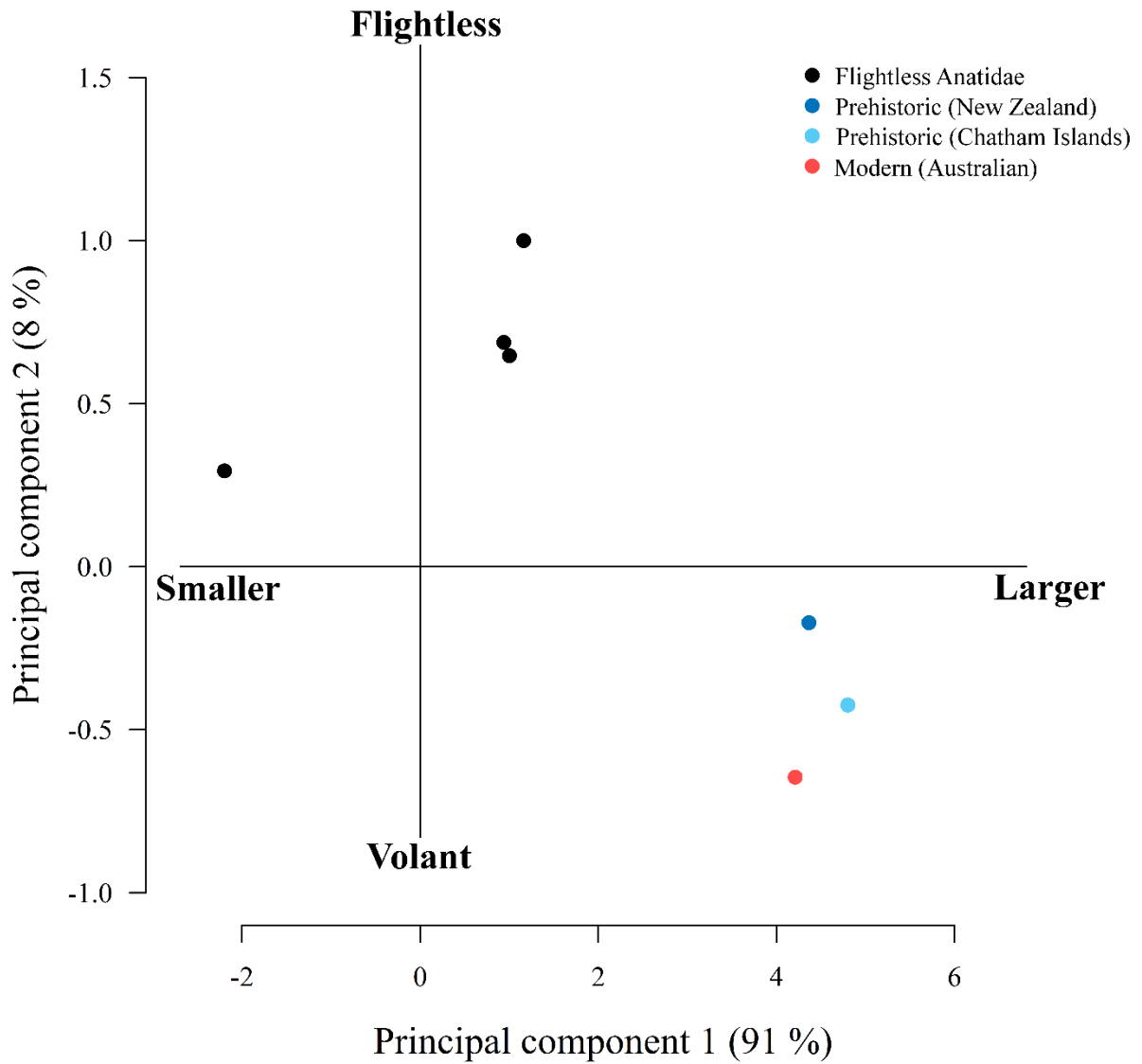
Figure S8 Principal Component Analysis of postcranial mean element length measurements (hum, ulna, cmc, fem and tmt) of modern (Australian) volant black swans, known flightless Anatidae (data sourced from Watanabe [9]), and prehistoric (NZ/CI) *Cygnus* swans of unknown flight ability.
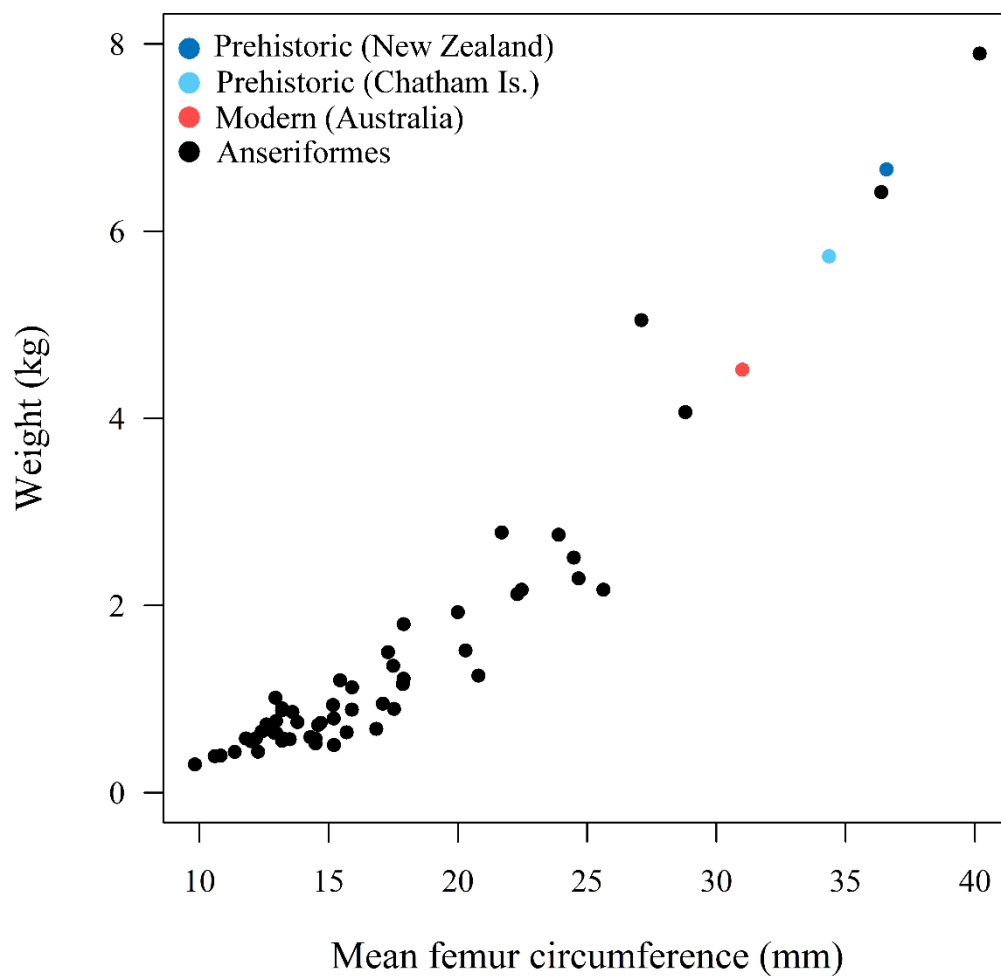
Figure S9 Relationship between mean body mass (in kg) and femora circumference of anseriforms. Data are from Dickison [10].